

WEIGHT-VARIANT LATENT CAUSAL MODELS

**Yuhang Liu¹, Zhen Zhang¹, Dong Gong², Mingming Gong³, Biwei Huang⁴
Anton van den Hengel¹, Kun Zhang⁵, Javen Qinfeng Shi¹**

¹ Australian Institute for Machine Learning, The University of Adelaide, Australia

² School of Computer Science and Engineering, The University of New South Wales, Australia

³ School of Mathematics and Statistics, The University of Melbourne, Australia

⁴ Halicioğlu Data Science Institute (HDSI), University of California San Diego, USA

⁵ Department of Philosophy, Carnegie Mellon University, USA

yuhang.liu01@adelaide.edu.au

ABSTRACT

Causal representation learning exposes latent high-level causal variables behind low-level observations, which has enormous potential for a set of downstream tasks of interest. Despite this, identifying the true latent causal representation from observed data is a great challenge. In this work we focus on identifying latent causal variables. To this end, we analysis three intrinsic properties in latent space, including transitivity, permutation and scaling. We show that the transitivity severely hinders the identifiability of latent causal variables, while permutation and scaling guide the direction of identifying latent causal variable. To break the transitivity, we assume the underlying latent causal relations to be linear Gaussian models, in which the weights, mean and variance of Gaussian noise are modulated by an additionally observed variable. Under these assumptions we theoretically show that the latent causal variables can be identifiable up to trivial permutation and scaling. Built on this theoretical result, we propose a novel method, termed Structural caUsAl Variational autoEncoder (SuaVE), which directly learns latent causal variables, together with the mapping from the latent causal variables to the observed ones. Experimental results on synthetic and real data demonstrate the identifiable result and the ability of the proposed SuaVE for learning latent causal variables.

1 INTRODUCTION

While there is no universal formal definition, one widely accepted feature of disentangled representations (Bengio et al., 2013) is that a change in one dimension corresponds to a change in one factor of variation in the underlying model of the data while being relatively invariant to changes in other factors. The underlying model is rarely available for interrogation, which makes learning disentangled representations challenging. Several excellent works for disentangled representation learning have been proposed that focus on enforcing independence over the latent variables that control the factors of variation (Higgins et al., 2017; Chen et al., 2018; Locatello et al., 2019; Kim & Mnih, 2018; Locatello et al., 2020). However, in many applications the latent variables are not statistically independent, which is at odds with the notion of disentanglement above, *i.e.*, foot length and body height exhibit strong positive correlation in observed data (Träuble et al., 2021).

Causal representation learning avoids the aforementioned limitation, as it aims to learn a representation that exposes the unknown high-level causal structural variables, and the relationships between them, from a set of low-level observations (Schölkopf et al., 2021). Unlike disentangled representation learning, it assumes that there may be causal relations among latent variables. In fact, disentangled representation learning can be viewed as a special case of causal representation learning where the latent variables have no causal relationships (Schölkopf et al., 2021). One of the most prominent additional capabilities for causal representation is the ability to make proper interventions or to make predictions under interventions (Pearl, 2000), which enables the generation of new samples that do not lie within the distribution of the observed data. This can be particularly useful to improve the generalization of the resulting model. Besides, causal representation has the ability to answer

counterfactual questions, *e.g.*, would a given patient have suffered heart failure if they had started exercising a year earlier (Schölkopf et al., 2021)?

Despite the above advantages, causal representation learning is a notoriously hard problem, because identifying the true latent causal model from observed data is impossible without strong assumptions. There are roughly three research lines in the identifiability of causal representation: 1) adapting supervised setting, *e.g.*, known latent causal graphs or/and labels (Kocaoglu et al., 2018; Yang et al., 2021; Von Kügelgen et al., 2021; Brehmer et al., 2022), 2) imposing sparse graphical conditions, *e.g.*, bottleneck graphical conditions (Adams et al., 2021; Xie et al., 2020; Lachapelle et al., 2021), 3) using temporal information (Yao et al., 2021; Lippe et al., 2022). A brief review will be introduced in Section 2. For the first line, under the setting where causal graphs or/and labels are known, the challenging identifiability problem in latent space has been transferred to an identifiability problem in observed space, for which some commonly-used function classes have been proven to be identifiable (Zhang & Hyvarinen, 2012; Peters et al., 2014). For the second line, many latent causal graphs in reality may be more or less arbitrary, beyond the pure sparse graph structure. The last line requires time-delayed temporal information or temporal intervened information among latent factors to identify the latent representation, which may be limited in time series data.

In this work, we explore a new line of research for the identifiability of causal representation, allowing the causal influences among latent causal variables to change. We focus on identifying latent causal variables, since once the distribution of latent causal variables is known, identifying causal graph structure is a well-studied problem with many solutions, *e.g.* additional noise models (Hoyer et al., 2008; Peters et al., 2014) or post-nonlinear models (Zhang & Hyvarinen, 2012). Our work is motivated by recent progress in the identifiability result of nonlinear ICA, which has shown that independent latent variables can be identifiable (Hyvarinen et al., 2019; Khemakhem et al., 2020), under mild assumptions. For example, independent latent variables are sampled from independent Gaussian variables whose mean and variance are modulated by an additionally observed variable \mathbf{u} . Due to the independence, *independent latent variables* in nonlinear ICA can be naturally corresponding to *independent latent noise variables* (exogenous Variables) in a latent causal model. Built on the identifiability result of nonlinear ICA, an interesting question appears, what are additional assumptions to recover the latent causal variables in a latent causal model? To answer this problem, we analysis three intrinsic properties in latent space, including transitivity, permutation and scaling, which implies the following insights. 1) The transitivity is the curse of identifiability of latent causal variables, which is the main challenge for the identifiability. 2) The permutation provides the blessing that we can always define a causal order for learning latent causal variable, avoiding troublesome directed acyclic graph (DAG) constraint. 3) The scaling and the permutation guide us to recover latent causal variables up to permutation and scaling, not up to exact values. To break the transitivity, we assume that the underlying causal representation can be modelled by weight-variate linear Gaussian models, in which the mean and variance of the Gaussian are changed by the additionally observed variable \mathbf{u} (guaranteeing the identifiability of independent noise variables), and the weights are also changed by the observed variable \mathbf{u} (additional assumption). With these assumptions, we show that the latent causal variables can be recover up to trivial permutation and scaling. The key of the identifiability result is that the weights (causal influences) among the latent causal variables are allowed to change. Intuitively, the changing causal influences enables us to obtain interventional observed data, which contributes the identifiability of latent causal variables. Built on this result, we further propose a novel method with the consistency of estimation for learning latent causal variables. Experimental results on synthetic and real data verify the proposed identifiability result and the effectiveness of the proposed model for learning the latent causal variables.

2 RELATED WORK

Due to the challenge in the identifiability of causal representation learning, most existing works handle this problem by imposing various assumptions. According to different assumptions, we summarize related works as following:

Supervised Causal Representation To simplify the challenge in the identifiability of causal representation, some works assume known latent causal graphs or labels. CausalGAN (Kocaoglu et al., 2018) requires a-priori knowledge of the structure of the causal graph of latent variables, which is a significant practical limitation. CausalVAE (Yang et al., 2021) needs additional labels to supervise the

learning of latent variables. Such labels are not commonly available, however, and manual labeling can be costly and error-prone. Von Kügelgen et al. (2021) use a known but non-trivial causal graph between content and style factors to study self-supervised causal representation learning. Brehmer et al. (2022) learn causal representation in a weakly supervised setting where we have access to data pairs, representing the system before and after a randomly chosen, unknown intervention.

Sparse Graphical Structure Most recent progress in the identifiability of latent causal discovery focuses on sparse graphical structure constraints (Silva et al., 2006; Shimizu et al., 2009; Anandkumar et al., 2013; Frot et al., 2019; Cai et al., 2019; Xie et al., 2020; 2022). Adams et al. (2021) summarize these sparse structure by a unified viewpoint where a sparser model that fits the observation is preferred. However, they often consider the linear settings where the causal relation between latent causal variables, and the relation between latent causal variables and observed variables are assumed linear, which can be easily violated in real-world applications. Very recently, Lachapelle et al. (2021) handles nonlinear causal relation between latent variables by assuming special sparse graphical structures. However, many latent causal graphs in reality may be more or less arbitrary, beyond the pure sparse graph structure. In contrast, our work assumes function class on latent variables, and does not restrict the graph structure over latent variables.

Temporal Information One can benefit from the temporal constraint that the effect cannot precede the cause, which helps to identify latent causal representation (Yao et al., 2021; Lippe et al., 2022; Yao et al., 2022). For example, Yao et al. (2021) recover latent causal variables and identify their relations from measured temporal data by using time-delayed causal relations among latent causal variables. Lippe et al. (2022) learn causal representations from temporal sequences, which requires the underlying causal factors to be intervened. Yao et al. (2021) identify latent causal variables in time series and by allowing the causal influences among the latent variables to change. In fact, all these works can be regarded as a special case of exploring the change of causal influences among latent variables in time series data. In contrast, this work is not restricted in time series, since the observed auxiliary variable u could represent time indices, domain indices, or almost any additional or side information, making it applicable to diverse problems and applications.

Besides, Kivva et al. (2021) considers a nonlinear setting for latent causal discovery. It assumes discrete latent causal variables that can be identifiable by a mixture oracle, while our work aims to handle continuous latent causal variables without such an oracle.

3 THREE INTRINSIC PROPERTIES IN LATENT SPACE

In this section we first connect nonlinear ICA and causal representation, by exploiting the correspondence between the independence of latent variables in nonlinear ICA and the independence of latent noise variables in causal representation. We then analysis three intrinsic properties in latent space, *e.g.*, transitivity, permutation and scaling, which reveals the curse and blessing of identifying latent causal variables.

3.1 RELATING CAUSAL REPRESENTATION WITH IDENTIFIABLE NONLINEAR ICA

Causal representation explores latent high-level causal model, which generates low-level observations by a nonlinear mapping. Formally, we assume that the observed x is caused by all latent causal variables z_i , and there is no edges from the observed x to the latent causal variables z_i . The causal structure graph among the latent causal variables z_i is unknown and could be a any directed acyclic graph. For each z_i in a causal representation, there is a corresponding latent noise variables n_i , as shown in Figure 1. Since the latent noise variables n_i are assumed to be independent in any causal system (Peters et al., 2017), it is natural to introduce recent progress in nonlinear ICA (Hyvarinen et al., 2019; Khemakhem et al., 2020), which has shown that the independent latent noise variables n_i can be identifiable by an additionally observed variable u , with relatively mild assumptions. For example, independent latent variables n_i

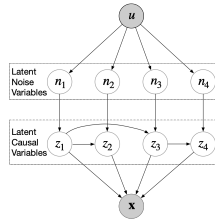


Figure 1: Causal representation with u .

are sampled from independent Gaussian distributions whose means and variances are modulated by the observed variable \mathbf{u} . Taking one step further, our goal is to recover the latent causal variables z_i . However, with the assumptions for the identifiability of latent noise variables n_i from nonlinear ICA, it is still insufficient to identify the latent causal variables z_i . We will discuss this in Section 3.2. Given this fact, an interesting problem is that what additional conditions are sufficient to recover the latent causal variables z_i , with the assumptions for the identifiable n_i . We will discuss this in Section 4.

3.2 TRANSITIVITY: THE CURSE OF IDENTIFYING LATENT CAUSAL VARIABLES

Even with the identifiable n_i , it is impossible to identify the latent causal variables z_i without additional assumptions. To interpret this point, for simplicity, let us consider the net effect of z_1 and z_2 on \mathbf{x} in Figure 1. According to the graph structure in Figure 1, assume that $z_1 := n_1$, $z_2 := z_1 + n_2$ and $\mathbf{x} := \mathbf{f}(z_1, z_2) + \varepsilon$ (case 1). Let us then consider the graph structure as shown in the left of Figure 2 where the edge of $z_1 \rightarrow z_2$ has been removed, and assume that $z_1 := n_1$,

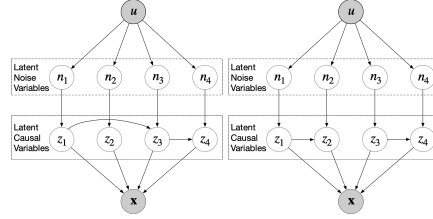


Figure 2: Two equivalent graph structures.

$z_2 := n_2$ and $\mathbf{x} := \mathbf{f} \circ \mathbf{g}(z_1, z_2) + \varepsilon$ where $\mathbf{g}(z_1, z_2) = [z_1, z_1 + z_2]$ (case 2). We can see that both case 1 and case 2 can generate the same observed data \mathbf{x} , which implies that we have two different equivalent causal structures to interpret the same observed data. Clearly, z_2 in both two equivalent causal structures are different, and thus z_2 is unidentifiable. Similarly, we can also cut the edge of $z_1 \rightarrow z_3$ in Figure 1, obtaining another equivalent causal graph as shown in the right of Figure 2. That is, we can have two different z_3 to interpret the same observed data, and thus z_3 is unidentifiable. Since there exists many different equivalent causal structures, the latent causal variables in Figure 1 is unidentifiable. Such result is because that the effect of z_1 on z_2 (or z_3) in latent space can be 'absorbed' by the nonlinear function from \mathbf{z} to \mathbf{x} . We term this property transitivity in this work. We will show how to handle this curse in Section 4. Before that, we introduce the other two properties in latent space, which assists in understanding the proposed identifiability result.

3.3 SCALING: THE INDETERMINACY OF RECOVERING LATENT CAUSAL VARIABLES

The scaling of the latent causal variables is also an intrinsic property in latent space. Again, let consider the net effect of z_1 and z_2 on \mathbf{x} in the Figure 1, and assume that $z_1 := n_1$, $z_2 := z_1 + n_2$ and $\mathbf{x} := \mathbf{f}(z_1, z_2) + \varepsilon$. Under this setting, if the value of z_1 is scaled by s , e.g. $s \times z_1$, we can easily obtained get the same observed data \mathbf{x} by: 1) letting $z_2 := \frac{1}{s} \times z_1 + n_2$ and 2) $\mathbf{x} := \mathbf{f} \circ \mathbf{g}(z_1, z_2) + \varepsilon$ where $\mathbf{g}(z_1, z_2) = [s \times z_1, z_1]$. This result is because that the scaling of the latent variables z_i can be 'absorbed' by the nonlinear function from \mathbf{z} to \mathbf{x} and the causal functions among the latent causal variables. Therefore, without side information to determine the values of the latent causal variables z_i , our goal is to identifying the latent causal variable up to scaling, not exactly recover the values. In general, this scaling do not affect identifying causal direction among the latent causal variables. We will further discuss this in Section 4.

3.4 PERMUTATION: THE BLESSING OF LATENT CAUSAL VARIABLES

Now we introduce the last important property in latent space, permutation. Assume that the semantic information for the four latent causal variables in the Figure 1 include: object size, object color, object shape and object location, and the causal relations are: 'object size causes object color, object size causes object shape, and object shape causes object location'. The correct topological order should be 'object size, object color, object shape and object location'. Due to lacking of the name for the four semantic information, we can arbitrarily name them. For example, 'object

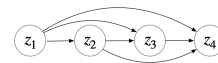


Figure 3: A Causal Supergraph.

size, object color, object shape and object location’ could be respectively named as ‘ z_4, z_2, z_1, z_3 ’, or ‘ z_1, z_2, z_3, z_4 ’, and so on. That is, the name of object size could be z_4 or z_1 , which implies that there exist permutations for a set of given latent causal variables. And without further side information, one can only recover latent causal variable up to permutation. In general, permutation is not important in many applications.

A key insight in this work is that we can always define a topological order, z_1, z_2, z_3, z_4 , as the correct topological order, by leveraging permutation. Under this setting, z_1 is enforced to denote the semantic information of the first latent variable in the true correct topological order, *e.g.* object size. Similarly, z_2 is enforced to denote the semantic information of the second latent variable in the true correct topological order, *e.g.* object color. As a result, z_1, z_2, z_3, z_4 can be the correct topological order. With the given topological order z_1, z_2, z_3, z_4 , we then can define a causal supergraph in latent space, as shown in Figure 3. Here a causal supergraph is defined a directed acyclic graph in which there is a directed edge for any two variables. This causal supergraph can naturally ensure a directed acyclic graph estimation in learning causal representation, avoiding DAG constraint. We will further discuss this in the proposed method for learning causal representation in Section 5.

4 IDENTIFIABLE LATENT CAUSAL VARIABLES WITH WEIGHT-VARIANT LINEAR GAUSSIAN MODELS

As mentioned in Section 3.2, the key problem for unidentifiable causal representation is the property of transitivity. Note that the transitivity is due to that the causal influences among the latent causal variables be ‘absorbed’ by the nonlinear mapping from \mathbf{z} to \mathbf{x} . To handle it, we propose that causal influences among latent causal variables are allowed to change by the additionally observed variable \mathbf{u} , as shown by the red line in Figure 4. Note that we here use the red lines to denote that causal influences are changed by \mathbf{u} , differing with the black lines that denote causal directions. Intuitively, variant causal influences among latent causal variables cannot be ‘absorbed’ by a invariant nonlinear mapping from \mathbf{z} to \mathbf{x} , resulting in identifiable causal representation. Formally, let $\mathbf{x} \in \mathbb{R}^d$ and $\mathbf{u} \in \mathbb{R}^m$ be two observed random variables, let $\mathbf{z} \in \mathbb{R}^n$ denote unknown latent causal variables. We assume the following causal model \mathbf{x} :

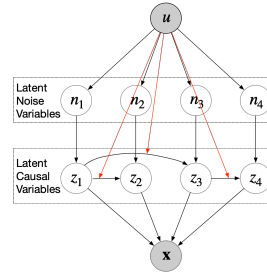


Figure 4: The proposed Latent Causal Model.

$$n_i \sim \mathcal{N}(\beta_{i,1}(\mathbf{u}), \beta_{i,2}(\mathbf{u})), \quad (1)$$

$$z_i := \boldsymbol{\lambda}_i^T(\mathbf{u})(\mathbf{z}) + n_i, \quad (2)$$

$$\mathbf{x} := \mathbf{f}(\mathbf{z}) + \varepsilon \quad (3)$$

where

- In Eq. (1), $\mathcal{N}(\beta_{i,1}(\mathbf{u}), \beta_{i,2}(\mathbf{u}))$ denote Gaussian noise with the mean $\beta_{i,1}(\mathbf{u})$ and the variance $\beta_{i,2}(\mathbf{u})$, both $\beta_{i,1}$ and $\beta_{i,2}$ can be nonlinear mappings,
- In Eq. (2), $\boldsymbol{\lambda}_i(\mathbf{u})$ denote the vector related to weights, *e.g.* $[\lambda_{1,i}(\mathbf{u}), \lambda_{2,i}(\mathbf{u}), \dots, \lambda_{n,i}(\mathbf{u})]$, and each $\lambda_{j,i}$ could be a nonlinear mapping. As mentioned in Section 3.4, we can define z_1, z_2, z_3, z_4 as the correct topological order, so that the corresponding weight matrix $\boldsymbol{\lambda} = [\boldsymbol{\lambda}_1(\mathbf{u}), \dots, \boldsymbol{\lambda}_n(\mathbf{u})]$ is the upper triangular matrix with zero-value diagonal elements.
- In Eq. (3), \mathbf{f} denote a nonlinear mapping, and ε is independent noise with probability density function, *e.g.*, $p_\varepsilon(\varepsilon)$.

Here we assume the underlying causal model is modelled by the linear model Eq. (2) where the weights is modulated by \mathbf{u} , we term it as weights-variant linear Gaussian model. This model is

a special linear Gaussian model, thus it defines a joint distribution $p(\mathbf{z})$ that is a jointly Gaussian distribution (Theorem 7.3, (Koller & Friedman, 2009)),

$$p_{(\boldsymbol{\lambda}, \boldsymbol{\beta})}(\mathbf{z}|\mathbf{u}) = \mathcal{N}(\boldsymbol{\mu}, \boldsymbol{\Sigma}), \quad (4)$$

where the mean $\boldsymbol{\mu}$ and the variance $\boldsymbol{\Sigma}$ can be obtained by the following rules:

$$\begin{aligned} \mu_i &= \boldsymbol{\lambda}_i^T(\mathbf{u})\boldsymbol{\mu} + \beta_{i,1}(\mathbf{u}), \\ \Sigma_{i,i} &= (\boldsymbol{\lambda}_i(\mathbf{u}) \odot \boldsymbol{\lambda}_i(\mathbf{u}))^T (\text{diag}(\boldsymbol{\Sigma})) + \beta_{i,2}(\mathbf{u}), \\ \Sigma_{j,i} &= \Sigma_{i,j} = (S_{i,j}^1 + \dots + S_{i,j}^b \dots + S_{i,j}^{n-1})\Sigma_{j,j}, \quad \text{for } i > j. \end{aligned} \quad (5)$$

where $\text{diag}(\boldsymbol{\Sigma})$ denote the vectorization of the diagonal elements of $\boldsymbol{\Sigma}$, $S_{i,j}^b$ is the sum of weight products along all b -step ($b = 1, 2, 3, \dots, n-1$) paths from node z_j to node z_i , which can be determined by the parameters $\boldsymbol{\lambda}$. This multi-variate Gaussian can be re-expressed by the following exponential family:

$$p_{(\mathbf{T}, \boldsymbol{\lambda}, \boldsymbol{\beta})}(\mathbf{z}|\mathbf{u}) = \frac{Q(\mathbf{z})}{Z(\boldsymbol{\lambda}, \boldsymbol{\beta}, \mathbf{u})} \exp\left(\mathbf{T}^T(\mathbf{z})\boldsymbol{\eta}(\mathbf{u})\right), \quad (6)$$

where the natural parameter $\boldsymbol{\eta}(\mathbf{u}) = [\boldsymbol{\Sigma}^{-1}\boldsymbol{\mu}; -\frac{1}{2}\text{vec}(\boldsymbol{\Sigma}^{-1})]$, the base measure $Q(\mathbf{z}) = (2\pi)^{-n/2}$, $Z(\boldsymbol{\lambda}, \boldsymbol{\beta}, \mathbf{u})$ denotes the normalizing constant, the sufficient statistic $\mathbf{T}(\mathbf{z}) = [\mathbf{z}; \text{vec}(\mathbf{z}\mathbf{z}^T)]$, where 'vec' denotes the vectorization of a matrix. Let k denotes the dimension of the sufficient statistic \mathbf{T} that is always considered to be minimal. Depending on different causal graph structures, the dimension of the sufficient statistic k may vary. For example, if we consider the graph structure in the Figure 1, the cross term z_2z_3 will not appear in Eq. equation 6, thus the sufficient statistic do not include z_2z_3 . Here we consider $2n \leq k \leq n + (n * (n + 1))/2$, in which $k = 2n$ is corresponding to that $\mathbf{T}(\mathbf{z}) = [\mathbf{z}; z_1^2, z_2^2, \dots, z_n^2]$ or there is no edges among the latent variables, while $k = n + (n * (n + 1))/2$ may be corresponding to a full-connected causal graph.

In summary, we have the following result:

Theorem 4.1 *Assume that we observe data sampled from a generative model defined according to equation 3, with parameters $(\mathbf{f}, \boldsymbol{\lambda}, \boldsymbol{\beta})$. Assume the following holds:*

- (i) *The set $\{\mathbf{x} \in \mathcal{X} | \varphi_\epsilon(\mathbf{x}) = 0\}$ has measure zero (i.e., has at most countable number of elements), where φ_ϵ is the characteristic function of the density p_ϵ .*
- (ii) *The function \mathbf{f} in equation 3 is bijective.*
- (iii) *The sufficient statistic includes the term $[z_1; z_2; \dots; z_n; z_1^2; z_2^2; \dots; z_n^2]$ at least.*
- (iv) *There exist $k + 1$ distinct points $\mathbf{u}_0, \mathbf{u}_1, \dots, \mathbf{u}_k$ such that the matrix*

$$\mathbf{L} = (\boldsymbol{\eta}(\mathbf{u}_1) - \boldsymbol{\eta}(\mathbf{u}_0), \dots, \boldsymbol{\eta}(\mathbf{u}_k) - \boldsymbol{\eta}(\mathbf{u}_0)) \quad (7)$$

of size $k \times k$ is invertible.

then we can recover the latent causal variables \mathbf{z} up to trivial permutation and linear scaling.

Intuitively, this identifiable result is due to the weight-variant linear Gaussian model Eq. equation 2. The variant weights 'affect' the causal influences among latent causal variables by the auxiliary observed variable \mathbf{u} , which can be regarded as intervention and contribute to the identifiability. A wrong causal structure over the latent variables will violate the assumed model class. As a challenging ill-posed problem, causal representation learning is known to be generally impossible without strong assumptions. The proposed weight-variant linear Gaussian model explores the possibility of identifiable causal representation learning, without any special causal graphical structure constraints. We believe that it can inspire future research direction in the identifiability of causal representation.

Up to now, our theorem guarantees that the recovered latent causal variables could be identifiable up to trivial permutation and linear scaling. With this result, identifiability of causal structure in *latent space* boils down to the identifiability of the causal structure in *observed space*. Recent progress in Ghassami et al. (2018) has shown that a linear model in observed space, under the conditions that the weights and/or the distribution of the exogenous noises may vary in multi domains, is identifiable.

And the causal direction can be identified by the fact that variance of cause is independent with the pair of variance of effect and the corresponding weights (Ghassami et al., 2018). Although there exist scaling for the recovered latent variables in our identifiability result, the scaling do not affect the fact for identifying the causal direction. As a result, we can conclude that the identifiability of latent causal variables implies the identifiability of causal structure in our setting.

5 LEARNING CAUSAL VARIABLES WITH WEIGHT-VARIANT LINEAR GAUSSIAN MODELS

Built on the identifiable result above, in this section we propose a structural causal variational autoencoder (SuaVE) to learn latent causal variables. We first propose a structural causal model prior relating to the proposed weight-variant linear Gaussian model. We then show how to incorporate the proposed prior into the traditional VAE framework. We finally give consistency result for the proposed SuaVE.

5.1 THE PROPOSED PRIOR ON LATENT CAUSAL VARIABLES

Since we can always define a super causal graph as shown in Figure 3 as mentioned in 3.4, the weight matrix λ is the upper triangular matrix. As a result, the causal model for the latent causal variables, e.g., Eq. equation 1 and Eq. equation 1, can be reformulated as the following probabilistic model.

$$p(\mathbf{z}|\mathbf{u}) = p(z_1|\mathbf{u}) \prod_{i=2}^n p(z_i|\mathbf{z}_{<i}, \mathbf{u}) = \prod_{i=1}^n \mathcal{N}(\mu_{z_i}, \delta_{z_i}^2), \quad (8)$$

where

$$\mu_{z_i} = \sum_{i' < i} \lambda_{i,i'}(\mathbf{u})(z_{i'}) + \beta_{i,1}(\mathbf{u}), \quad \delta_{z_i}^2 = \beta_{i,2}(\mathbf{u}). \quad (9)$$

The proposed prior naturally ensures a directed acyclic graph estimation, avoiding DAG constraint. In contrast, traditional methods, *i.e.* CausalVAE (Yang et al., 2021), employ a relaxed DAG constraint proposed by (Zheng et al., 2018) to estimate the causal graph, which may result in a cyclic graph estimation due to the inappropriate setting of the regularization hyper parameter.

5.2 THE PROPOSED SUAWE FOR LEARNING LATENT CAUSAL VARIABLES

The nature of the proposed prior equation 8 gives rise to the following variational posterior:

$$q(\mathbf{z}|\mathbf{x}, \mathbf{u}) = q(z_1|\mathbf{x}, \mathbf{u}) \prod_{i=2}^n q(z_i|\mathbf{z}_{<i}, \mathbf{x}, \mathbf{u}) = \prod_{i=1}^n \mathcal{N}(\mu'_{z_i}, \delta'^2_{z_i}), \quad (10)$$

where:

$$\mu'_{z_i} = \sum_{i' < i} \lambda'_{i,i'}(\mathbf{u})z_{i'} + \beta'_{i,1}(\mathbf{x}, \mathbf{u}), \quad \delta'^2_{z_i} = \beta'_{i,2}(\mathbf{x}, \mathbf{u}). \quad (11)$$

Thus, we arrive at a simple objective:

$$\max \mathbb{E}_{q(\mathbf{z}|\mathbf{x}, \mathbf{u})} (p(\mathbf{x}|\mathbf{z}, \mathbf{u})) - D_{KL}(q(\mathbf{z}|\mathbf{x}, \mathbf{u})||p(\mathbf{z}|\mathbf{u})), \quad (12)$$

where D_{KL} denotes Kullback–Leibler divergence. Note that the proposed SuaVE is totally different from hierarchical VAE models (Kingma et al., 2016; Sønderby et al., 2016; Maaløe et al., 2019; Vahdat & Kautz, 2020) in that the former has rigorous theoretical justification for identifiability, while the latter has no such supports without further assumptions. Besides, the theoretical justification implies **the consistency of estimation** for the proposed SuaVE as follows:

Theorem 5.1 *Assume the following holds:*

- (i) *The variational distributions equation 10 contains the true posterior distribution $p_{\mathbf{f}, \mathbf{T}, \lambda, \beta}(\mathbf{z}|\mathbf{x}, \mathbf{u})$.*
- (ii) *We maximize the objective function: $\max \mathbb{E}_{q(\mathbf{z}|\mathbf{x}, \mathbf{u})} (p(\mathbf{x}|\mathbf{z}, \mathbf{u})) - D_{KL}(q(\mathbf{z}|\mathbf{x}, \mathbf{u})||p(\mathbf{z}|\mathbf{u}))$.*

then in the limit of infinite data, the proposed SuaVE learns the true parameters $\theta = (\mathbf{f}, \mathbf{T}, \lambda, \beta)$ up to the equivalence class with permutation and scaling.

6 EXPERIMENTS

6.1 SYNTHETIC DATA

Data We first conduct experiments on synthetic data, generated by the following process: we divide the latent noise variables into M segments, each segment corresponds to one conditional variable \mathbf{u} as the segment label. Within each segment, we first sample the mean $\beta_{i,1}$ and variance $\beta_{i,2}$ from uniform distributions $[-2, 2]$ and $[0.01, 1]$, respectively. We then sample the weights $\lambda_{i,j}$ from uniform distributions $[0.1, 2]$. Then for each segment, we generate the latent causal samples according to the generative model equation 3. Finally, we obtain the observed data samples \mathbf{x} by an invertible nonlinear mapping. More details can be found in Appendix.

Comparison We compare the proposed method with identifiable VAE (iVAE) Khemakhem et al. (2020), β -VAE Higgins et al. (2017), CausalVAE Yang et al. (2021), and vanilla VAE Kingma & Welling (2013). Among them, iVAE has been proven to be identifiable so that it is able to learn the true independent noise variables with some assumptions. While β -VAE has no theoretical support, it has been widely used in various disentanglement tasks. Note that all those two methods assume that the latent variables are independent, and thus they cannot model the relationship among latent variables. To make a fair comparison in the unsupervised setting, we implement an unsupervised version of CausalVAE, which is not identifiable.

Performance metric Since the proposed method can recover the latent causal variables up to trivial permutation and linear scaling, we compute the mean of the Pearson correlation coefficient (MPC) to evaluate the performance of our proposed method. The Pearson correlation coefficient is a measure of linear correlation between the true latent causal variables and the recovered latent causal variables. Note that the Pearson coefficient is suitable for iVAE, since it has been shown that iVAE can also recover the latent noise variables up to linear scaling under the setting where mean and variance of the latent noise variables are changed by \mathbf{u} (Sorrenson et al., 2020). To remove the permutation effect, following Khemakhem et al. (2020), we first calculate all pairs of correlation, then solve a linear sum assignment problem to obtain the final results. A high correlation coefficient means that we successfully identified the true parameters and recovered the true variables, up to component-wise linear transformations.

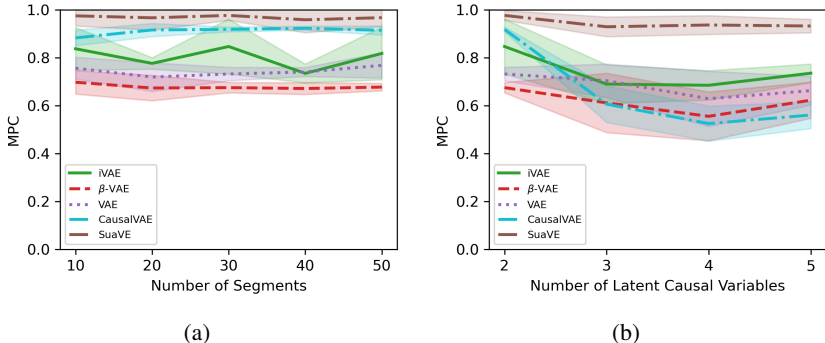


Figure 5: Performances of the proposed SuaVE in comparison to iVAE, β -VAE, VAE and CausalVAE in recovering the latent causal variables on synthetic data with different numbers of segments (a), and with different numbers of the latent causal variables (b). The proposed SuaVE obtain the best MPC, compared with the others.

Results We compared the performance of the proposed SuaVE to some variants of VAE mentioned above. We used the same network architecture for encoder and decoder parts in all these models. In particular, we add a sub-network to model the conditional prior in both iVAE and the proposed SuaVE. We further assign an linear SCM sub-network to model the relations among latent causal variables in the proposed SuaVE. We trained these 5 models on the dataset described above, with different numbers of segments and different numbers of latent causal variables. For each method, we

use 5 different random seeds for data sampling. Figure 5 (a) shows the performance on two latent causal variables with different numbers of segment. The proposed SuaVE obtains the score 0.96 approximately for all the different numbers of segment. In contrast, β -VAE, VAE and CausalVAE fail to achieve a good estimation of the true latent variables, since they are not identifiable. iVAE obtains unsatisfactory results, since its theory only holds for i.i.d. latent variables. Figure 5 (b) shows the performance in recovering latent causal variables on synthetic data with different numbers of the latent causal variables.

6.2 FMRI DATA

Following Ghassami et al. (2018), we applied the proposed method to fMRI hippocampus dataset (Laumann & Poldrack, 2015), which contains signals from six separate brain regions: perirhinal cortex (PRC), parahippocampal cortex (PHC), entorhinal cortex (ERC), subiculum (Sub), CA1, and CA3/Dentate Gyrus (CA3) in the resting states on the same person in 84 successive days. Since we are interested in recovering latent causal variables, we treat the six signals as latent causal variables by applying a random nonlinear mapping on them to obtain observed data. We then applied various methods on the observed data to recover the six signals. Figure 6 shows the performance of the proposed SuaVE in comparison to iVAE, β -VAE, VAE and CausalVAE in recovering the latent six signals. Figure 6 shows the recovered latent six signals (Blue) and the true ones (Red) within one day by the proposed SuaVE.

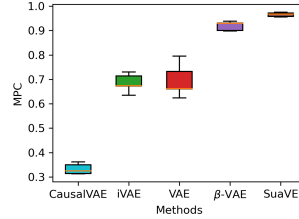


Figure 6: Performance on fMRI Data.

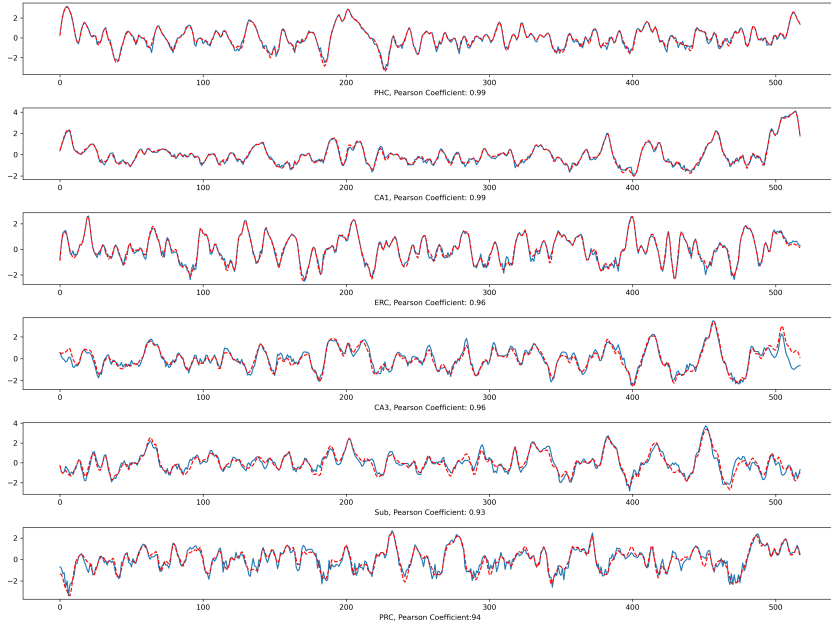


Figure 7: Recovered latent six signals (Blue) and the true ones (Red) within one day by the proposed SuaVE.

7 CONCLUSION

Causal representation is known to be generally impossible without strong assumptions, due to unidentifiability. Motivated by recent progress in the identifiability of nonlinear iCA, we analysis the intrinsic three properties in latent space, *e.g.*, transitivity, permutation and scaling, which provides

deep insights for the curse and blessing of identifying latent causal variables. To break the curse of the transitivity, we propose a novel line of research, allowing the causal influences among the latent causal variables to change by the additionally observed variable. Concretely, we propose weight-variant linear Gaussian model to capture the underlying causal relations among latent causal variables, and show that the model can recover the latent causal variables up to simple permutation and scaling. We then propose a novel method, termed SuaVE, which has proved to be a consistent estimator, to learn latent causal variables. Experiments on synthetic and real data show the advantages of our theoretical results and the performance of the proposed SuaVE. Future work may include exploring more general linear models and nonlinear models to model the causal relations among latent causal variables.

REFERENCES

- Jeffrey Adams, Niels Hansen, and Kun Zhang. Identification of partially observed linear causal models: Graphical conditions for the non-gaussian and heterogeneous cases. In *NeurIPS*, 2021.
- Animashree Anandkumar, Daniel Hsu, Adel Javanmard, and Sham Kakade. Learning linear bayesian networks with latent variables. In *ICML*, pp. 249–257, 2013.
- Yoshua Bengio, Aaron Courville, and Pascal Vincent. Representation learning: A review and new perspectives. *IEEE TPAMI*, 35(8):1798–1828, 2013.
- Johann Brehmer, Pim De Haan, Phillip Lippe, and Taco Cohen. Weakly supervised causal representation learning. *arXiv preprint arXiv:2203.16437*, 2022.
- Ruichu Cai, Feng Xie, Clark Glymour, Zhifeng Hao, and Kun Zhang. Triad constraints for learning causal structure of latent variables. In *NeurIPS*, 2019.
- Ricky TQ Chen, Xuechen Li, Roger Grosse, and David Duvenaud. Isolating sources of disentanglement in vaes. In *NeurIPS*, 2018.
- Benjamin Frot, Preetam Nandy, and Marloes H Maathuis. Robust causal structure learning with some hidden variables. *Journal of the Royal Statistical Society: Series B (Statistical Methodology)*, 81(3):459–487, 2019.
- AmirEmad Ghassami, Negar Kiyavash, Biwei Huang, and Kun Zhang. Multi-domain causal structure learning in linear systems. *Advances in neural information processing systems*, 31, 2018.
- I. Higgins, Loïc Matthey, A. Pal, Christopher P. Burgess, Xavier Glorot, M. Botvinick, S. Mohamed, and Alexander Lerchner. beta-vae: Learning basic visual concepts with a constrained variational framework. In *ICLR*, 2017.
- Patrik O Hoyer, Dominik Janzing, Joris M Mooij, Jonas Peters, Bernhard Schölkopf, et al. Nonlinear causal discovery with additive noise models. In *NeurIPS*, volume 21, pp. 689–696. Citeseer, 2008.
- Aapo Hyvarinen, Hiroaki Sasaki, and Richard Turner. Nonlinear ica using auxiliary variables and generalized contrastive learning. In *The 22nd International Conference on Artificial Intelligence and Statistics*, pp. 859–868. PMLR, 2019.
- Ilyes Khemakhem, Diederik Kingma, Ricardo Monti, and Aapo Hyvarinen. Variational autoencoders and nonlinear ica: A unifying framework. In *AISTAS*, pp. 2207–2217. PMLR, 2020.
- Hyunjik Kim and Andriy Mnih. Disentangling by factorising. In *ICML*, 2018.
- Diederik P Kingma and Max Welling. Auto-encoding variational bayes. *arXiv preprint arXiv:1312.6114*, 2013.
- Durk P Kingma, Tim Salimans, Rafal Jozefowicz, Xi Chen, Ilya Sutskever, and Max Welling. Improved variational inference with inverse autoregressive flow. In *NeurIPS*, volume 29, pp. 4743–4751, 2016.
- Bohdan Kivva, Goutham Rajendran, Pradeep Ravikumar, and Bryon Aragam. Learning latent causal graphs via mixture oracles. *NeurIPS*, 2021.

- Murat Kocaoglu, Christopher Snyder, Alexandros G Dimakis, and Sriram Vishwanath. CausalGAN: Learning causal implicit generative models with adversarial training. In *ICLR*, 2018.
- Daphne Koller and Nir Friedman. *Probabilistic graphical models: principles and techniques*. MIT press, 2009.
- Sébastien Lachapelle, Pau Rodríguez López, Yash Sharma, Katie Everett, Rémi Le Priol, Alexandre Lacoste, and Simon Lacoste-Julien. Disentanglement via mechanism sparsity regularization: A new principle for nonlinear ica. *arXiv preprint arXiv:2107.10098*, 2021.
- Timothy O. Laumann and Russell A. Poldrack, 2015. URL <https://openfmri.org/dataset/ds000031/>.
- Phillip Lippe, Sara Magliacane, Sindy Löwe, Yuki M Asano, Taco Cohen, and Stratis Gavves. Citris: Causal identifiability from temporal intervened sequences. In *International Conference on Machine Learning*, pp. 13557–13603. PMLR, 2022.
- Francesco Locatello, Stefan Bauer, Mario Lucic, Gunnar Raetsch, Sylvain Gelly, Bernhard Schölkopf, and Olivier Bachem. Challenging common assumptions in the unsupervised learning of disentangled representations. In *ICML*, 2019.
- Francesco Locatello, Ben Poole, Gunnar Rätsch, Bernhard Schölkopf, Olivier Bachem, and Michael Tschannen. Weakly-supervised disentanglement without compromises. In *ICML*, 2020.
- Lars Maaløe, Marco Fraccaro, Valentin Liévin, and Ole Winther. Biva: A very deep hierarchy of latent variables for generative modeling. In *NeurIPS*, 2019.
- J. Pearl. *Causality: Models, Reasoning, and Inference*. Cambridge University Press, Cambridge, 2000.
- Jonas Peters, Joris M. Mooij, Dominik Janzing, and Bernhard Schölkopf. Causal discovery with continuous additive noise models. *JMLR*, 15(58):2009–2053, 2014.
- Jonas Peters, Dominik Janzing, and Bernhard Schölkopf. *Elements of Causal Inference: Foundations and Learning Algorithms*. The MIT Press, 2017.
- Bernhard Schölkopf, Francesco Locatello, Stefan Bauer, Nan Rosemary Ke, Nal Kalchbrenner, Anirudh Goyal, and Yoshua Bengio. Toward causal representation learning. *Proceedings of the IEEE*, 109(5):612–634, 2021.
- Shohei Shimizu, Patrik O Hoyer, and Aapo Hyvärinen. Estimation of linear non-gaussian acyclic models for latent factors. *Neurocomputing*, 72(7-9):2024–2027, 2009.
- Ricardo Silva, Richard Scheines, Clark Glymour, Peter Spirtes, and David Maxwell Chickering. Learning the structure of linear latent variable models. *JMLR*, 7(2), 2006.
- Casper Kaae Sønderby, Tapani Raiko, Lars Maaløe, Søren Kaae Sønderby, and Ole Winther. Ladder variational autoencoders. In *NeurIPS*, 2016.
- Peter Sorrenson, Carsten Rother, and Ullrich Köthe. Disentanglement by nonlinear ica with general incompressible-flow networks (gin). *arXiv preprint arXiv:2001.04872*, 2020.
- Frederik Träuble, Elliot Creager, Niki Kilbertus, Francesco Locatello, Andrea Dittadi, Anirudh Goyal, Bernhard Schölkopf, and Stefan Bauer. On disentangled representations learned from correlated data. In *ICML*, pp. 10401–10412. PMLR, 2021.
- Arash Vahdat and Jan Kautz. Nvae: A deep hierarchical variational autoencoder. In *NeurIPS*, 2020.
- Julius Von Kügelgen, Yash Sharma, Luigi Gresele, Wieland Brendel, Bernhard Schölkopf, Michel Besserve, and Francesco Locatello. Self-supervised learning with data augmentations provably isolates content from style. In *Advances in neural information processing systems*, 2021.
- Feng Xie, Ruichu Cai, Biwei Huang, Clark Glymour, Zhifeng Hao, and Kun Zhang. Generalized independent noise condition for estimating latent variable causal graphs. In *NeurIPS*, 2020.

- Feng Xie, Biwei Huang, Zhengming Chen, Yangbo He, Zhi Geng, and Kun Zhang. Identification of linear non-gaussian latent hierarchical structure. In *International Conference on Machine Learning*, pp. 24370–24387. PMLR, 2022.
- Mengyue Yang, Furui Liu, Zhitang Chen, Xinwei Shen, Jianye Hao, and Jun Wang. Causalvae: Structured causal disentanglement in variational autoencoder. In *CVPR*, 2021.
- Weiran Yao, Yuewen Sun, Alex Ho, Changyin Sun, and Kun Zhang. Learning temporally causal latent processes from general temporal data. *arXiv preprint arXiv:2110.05428*, 2021.
- Weiran Yao, Guangyi Chen, and Kun Zhang. Learning latent causal dynamics. *arXiv preprint arXiv:2202.04828*, 2022.
- Kun Zhang and Aapo Hyvarinen. On the identifiability of the post-nonlinear causal model. *arXiv preprint arXiv:1205.2599*, 2012.
- Xun Zheng, Bryon Aragam, Pradeep Ravikumar, and Eric P Xing. Dags with no tears: Continuous optimization for structure learning. In *NeurIPS*, 2018.

A APPENDIX

A.1 THE PROOF OF THEOREM 4.1

The proof of Theorem 4.1 is done in three steps. The steps I is the same as nonlinear ICA Khemakhem et al. (2020), which builds a connection between any two different solutions by using a simple convolutional trick made possible by assumption (i). The step II consists of building a linear connection between any two different solutions by assumptions (iv). This step is different with nonlinear ICA Khemakhem et al. (2020) in that we employ the assumptions of multivariate Gaussian as Eq. equation 6, which can model the linear causal relations among the latent causal variables, while nonlinear ICA Khemakhem et al. (2020) assumes independent noise variables. The step III shows that we can recover latent causal variables up to linear scaling and permutation by the identity theorem for polynomials and assumptions (iii).

Step I: Suppose we have two sets of parameters $\theta = (\mathbf{f}, \mathbf{T}, \boldsymbol{\lambda}, \boldsymbol{\beta})$ and $\hat{\theta} = (\hat{\mathbf{f}}, \hat{\mathbf{T}}, \hat{\boldsymbol{\lambda}}, \hat{\boldsymbol{\beta}})$ such that $p_{(\mathbf{f}, \mathbf{T}, \boldsymbol{\lambda}, \boldsymbol{\beta})}(\mathbf{x}|\mathbf{u}) = p_{(\hat{\mathbf{f}}, \hat{\mathbf{T}}, \hat{\boldsymbol{\lambda}}, \hat{\boldsymbol{\beta}})}(\mathbf{x}|\mathbf{u})$ for all pairs (\mathbf{x}, \mathbf{u}) . Then:

$$\int p_{(\mathbf{T}, \boldsymbol{\lambda}, \boldsymbol{\beta})}(\mathbf{z}|\mathbf{u})p_{(\mathbf{f})}(\mathbf{x}|\mathbf{z}) d\mathbf{z} = \int p_{(\hat{\mathbf{T}}, \hat{\boldsymbol{\lambda}}, \hat{\boldsymbol{\beta}})}(\mathbf{z}|\mathbf{u})p_{(\hat{\mathbf{f}})}(\mathbf{x}|\mathbf{z}) d\mathbf{z} \quad (13)$$

$$\Rightarrow \int p_{(\mathbf{T}, \boldsymbol{\lambda}, \boldsymbol{\beta})}(\mathbf{z}|\mathbf{u})p_{\varepsilon}(\mathbf{x} - \mathbf{f}(\mathbf{z})) d\mathbf{z} = \int p_{(\hat{\mathbf{T}}, \hat{\boldsymbol{\lambda}}, \hat{\boldsymbol{\beta}})}(\mathbf{z}|\mathbf{u})p_{\varepsilon}(\mathbf{x} - \hat{\mathbf{f}}(\mathbf{z})) d\mathbf{z} \quad (14)$$

$$\Rightarrow \int p_{(\mathbf{T}, \boldsymbol{\lambda}, \boldsymbol{\beta})}(\mathbf{f}^{-1}(\bar{\mathbf{x}})|\mathbf{u})\text{vol}J_{\mathbf{f}^{-1}}(\bar{\mathbf{x}})p_{\varepsilon}(\mathbf{x} - \bar{\mathbf{x}}) d\bar{\mathbf{x}} = \int p_{(\hat{\mathbf{T}}, \hat{\boldsymbol{\lambda}}, \hat{\boldsymbol{\beta}})}(\hat{\mathbf{f}}^{-1}(\bar{\mathbf{x}}|\mathbf{u}))\text{vol}\hat{J}_{\hat{\mathbf{f}}^{-1}}(\bar{\mathbf{x}})p_{\varepsilon}(\mathbf{x} - \bar{\mathbf{x}}) d\bar{\mathbf{x}} \quad (15)$$

$$\Rightarrow \int \hat{p}_{(\mathbf{T}, \boldsymbol{\lambda}, \boldsymbol{\beta}, \mathbf{f}, \mathbf{u})}(\bar{\mathbf{x}})p_{\varepsilon}(\mathbf{x} - \bar{\mathbf{x}}) d\bar{\mathbf{x}} = \int \hat{p}_{(\hat{\mathbf{T}}, \hat{\boldsymbol{\lambda}}, \hat{\boldsymbol{\beta}}, \hat{\mathbf{f}}, \mathbf{u})}(\bar{\mathbf{x}})p_{\varepsilon}(\mathbf{x} - \bar{\mathbf{x}}) d\bar{\mathbf{x}} \quad (16)$$

$$\Rightarrow (\hat{p}_{(\mathbf{T}, \boldsymbol{\lambda}, \boldsymbol{\beta}, \mathbf{f}, \mathbf{u})} * p_{\varepsilon})(\mathbf{x}) = (\hat{p}_{(\hat{\mathbf{T}}, \hat{\boldsymbol{\lambda}}, \hat{\boldsymbol{\beta}}, \hat{\mathbf{f}}, \mathbf{u})} * p_{\varepsilon})(\mathbf{x}) \quad (17)$$

$$\Rightarrow F[\hat{p}_{(\mathbf{T}, \boldsymbol{\lambda}, \boldsymbol{\beta}, \mathbf{f}, \mathbf{u})}](\omega)\varphi_{\varepsilon}(\omega) = F[\hat{p}_{(\hat{\mathbf{T}}, \hat{\boldsymbol{\lambda}}, \hat{\boldsymbol{\beta}}, \hat{\mathbf{f}}, \mathbf{u})}](\omega)\varphi_{\varepsilon}(\omega) \quad (18)$$

$$\Rightarrow F[\hat{p}_{(\mathbf{T}, \boldsymbol{\lambda}, \boldsymbol{\beta}, \mathbf{f}, \mathbf{u})}](\omega) = F[\hat{p}_{(\hat{\mathbf{T}}, \hat{\boldsymbol{\lambda}}, \hat{\boldsymbol{\beta}}, \hat{\mathbf{f}}, \mathbf{u})}](\omega) \quad (19)$$

$$\Rightarrow \hat{p}_{(\mathbf{T}, \boldsymbol{\lambda}, \boldsymbol{\beta}, \mathbf{f}, \mathbf{u})}(\mathbf{x}) = \hat{p}_{(\hat{\mathbf{T}}, \hat{\boldsymbol{\lambda}}, \hat{\boldsymbol{\beta}}, \hat{\mathbf{f}}, \mathbf{u})}(\mathbf{x}) \quad (20)$$

where:

- in equation equation 15, J denotes the Jacobian, and we introduce here the volume of a matrix denoted $\text{vol}J$ as the product of the singular values of J . When J is full column rank, $\text{vol}J = \sqrt{|\det J^T J|}$, and when J is invertible, $\text{vol}J = |\det J|$. We made the change of variable $\bar{\mathbf{x}} = \mathbf{f}(\mathbf{z})$ on the left hand side, and $\bar{\mathbf{x}} = \hat{\mathbf{f}}(\mathbf{z})$ on the right hand side.
- in equation equation 16, we used $*$ for the convolution operator.
- in equation equation 18, we used $F[\cdot]$ to designate the Fourier transform.
- in equation equation 19, we dropped φ_{ε} from both sides as it is non-zero almost everywhere (by assumption (i)).

Step II By taking the logarithm on both sides of equation equation 20 and replacing $p_{(\mathbf{T}, \boldsymbol{\lambda}, \boldsymbol{\beta}, \mathbf{G})}$ by its expression from equation 6, we have:

$$\log \text{vol}J_{\mathbf{f}^{-1}}(\mathbf{x}) + \mathbf{T}^T(\mathbf{f}^{-1}(\mathbf{x}))\boldsymbol{\eta}(\mathbf{u}) - \log Z(\boldsymbol{\lambda}, \boldsymbol{\beta}, \mathbf{u}) = \quad (21)$$

$$\log \text{vol}J_{\hat{\mathbf{f}}^{-1}}(\mathbf{x}) + \hat{\mathbf{T}}^T(\hat{\mathbf{f}}^{-1}(\mathbf{x}))\hat{\boldsymbol{\eta}}(\mathbf{u}) - \log \hat{Z}(\hat{\boldsymbol{\lambda}}, \hat{\boldsymbol{\beta}}, \mathbf{u}). \quad (22)$$

Let $\mathbf{u}_0, \mathbf{u}_1, \dots, \mathbf{u}_{k+1}$ be the points provided by assumption (iv) of the Theorem. Similar to nonlinear ICA Khemakhem et al. (2020), we plug each of those $\mathbf{u}_l, l = 1, \dots, k$ in equation 22 to obtain $k + 1$ equations. We define $\bar{\boldsymbol{\eta}}(\mathbf{u}) = \boldsymbol{\eta}(\mathbf{u}) - \boldsymbol{\eta}(\mathbf{u}_0)$, and subtract the first equation for \mathbf{u}_0 from the remaining k equations. For example, for \mathbf{u}_0 and \mathbf{u}_k we have two equations:

$$\log \text{vol}J_{\mathbf{f}^{-1}}(\mathbf{x}) + \mathbf{T}^T(\mathbf{f}^{-1}(\mathbf{x}))\boldsymbol{\eta}(\mathbf{u}_0) - \log Z(\boldsymbol{\lambda}, \boldsymbol{\beta}, \mathbf{u}_0) = \quad (23)$$

$$\log \text{vol}J_{\hat{\mathbf{f}}^{-1}}(\mathbf{x}) + \hat{\mathbf{T}}^T(\hat{\mathbf{f}}^{-1}(\mathbf{x}))\hat{\boldsymbol{\eta}}(\mathbf{u}_0) - \log \hat{Z}(\hat{\boldsymbol{\lambda}}, \hat{\boldsymbol{\beta}}, \mathbf{u}_0),$$

and

$$\begin{aligned} \log \text{vol} J_{\mathbf{f}^{-1}}(\mathbf{x}) + \mathbf{T}^T(\mathbf{f}^{-1}(\mathbf{x}))\boldsymbol{\eta}(\mathbf{u}_{nk}) - \log Z(\boldsymbol{\lambda}, \boldsymbol{\beta}, \mathbf{u}_{nk}) = \\ \log \text{vol} J_{\hat{\mathbf{f}}^{-1}}(\mathbf{x}) + \hat{\mathbf{T}}^T(\hat{\mathbf{f}}^{-1}(\mathbf{x}))\hat{\boldsymbol{\eta}}(\mathbf{u}_{nk}) - \log \hat{Z}(\hat{\boldsymbol{\lambda}}, \hat{\boldsymbol{\beta}}, \mathbf{u}_{nk}), \end{aligned} \quad (24)$$

Using equation equation 24 subtracts equation equation 23, removing the terms that do not include \mathbf{u} , we have:

$$\begin{aligned} \mathbf{T}^T(\mathbf{f}^{-1}(\mathbf{x}))\boldsymbol{\eta}(\mathbf{u}_k) - \log Z(\boldsymbol{\lambda}, \boldsymbol{\beta}, \mathbf{u}_k) - \mathbf{T}^T(\mathbf{f}^{-1}(\mathbf{x}))\boldsymbol{\eta}(\mathbf{u}_0) + \log Z(\boldsymbol{\lambda}, \boldsymbol{\beta}, \mathbf{u}_0) \\ = \hat{\mathbf{T}}^T(\hat{\mathbf{f}}^{-1}(\mathbf{x}))\hat{\boldsymbol{\eta}}(\mathbf{u}_k) - \log \hat{Z}(\hat{\boldsymbol{\lambda}}, \hat{\boldsymbol{\beta}}, \mathbf{u}_k) - \hat{\mathbf{T}}^T(\hat{\mathbf{f}}^{-1}(\mathbf{x}))\hat{\boldsymbol{\eta}}(\mathbf{u}_0) - \log \hat{Z}(\hat{\boldsymbol{\lambda}}, \hat{\boldsymbol{\beta}}, \mathbf{u}_0). \end{aligned} \quad (25)$$

As a result, we arrive at:

$$\langle \mathbf{T}(\mathbf{f}^{-1}(\mathbf{x})), \bar{\boldsymbol{\eta}}(\mathbf{u}_l) \rangle + \log \frac{Z(\boldsymbol{\lambda}, \boldsymbol{\beta}, \mathbf{u}_0)}{Z(\boldsymbol{\lambda}, \boldsymbol{\beta}, \mathbf{u}_l)} = \langle \hat{\mathbf{T}}(\hat{\mathbf{f}}^{-1}(\mathbf{x})), \bar{\boldsymbol{\eta}}(\mathbf{u}_l) \rangle + \log \frac{\hat{Z}(\hat{\boldsymbol{\lambda}}, \hat{\boldsymbol{\beta}}, \mathbf{u}_0)}{\hat{Z}(\hat{\boldsymbol{\lambda}}, \hat{\boldsymbol{\beta}}, \mathbf{u}_l)}. \quad (26)$$

Let \mathbf{L} be the matrix defined in equation equation 7 in assumption (iv), and $\hat{\mathbf{L}}$ similarly ($\hat{\mathbf{L}}$ is not necessarily invertible). Define $b_l = \log \frac{\hat{Z}(\hat{\boldsymbol{\lambda}}, \hat{\boldsymbol{\beta}}, \mathbf{u}_0) Z(\boldsymbol{\lambda}, \boldsymbol{\beta}, \mathbf{u}_l)}{Z(\boldsymbol{\lambda}, \boldsymbol{\beta}, \mathbf{u}_0) \hat{Z}(\hat{\boldsymbol{\lambda}}, \hat{\boldsymbol{\beta}}, \mathbf{u}_l)}$ and \mathbf{b} the vector for b_l . Expressing equation 26 for all points \mathbf{u}_l in matrix form, we get:

$$\mathbf{L}^T \mathbf{T}(\mathbf{f}^{-1}(\mathbf{x})) = \hat{\mathbf{L}}^T \hat{\mathbf{T}}(\hat{\mathbf{f}}^{-1}(\mathbf{x})) + \mathbf{b}. \quad (27)$$

We multiply both sides of equation equation 27 by the inverse of \mathbf{L}^T to find:

$$\mathbf{T}(\mathbf{f}^{-1}(\mathbf{x})) = \mathbf{A} \hat{\mathbf{T}}(\hat{\mathbf{f}}^{-1}(\mathbf{x})) + \mathbf{c}, \quad (28)$$

where $\mathbf{A} = (\mathbf{L}^T)^{-1} \hat{\mathbf{L}}^T$ and $\mathbf{c} = (\mathbf{L}^T)^{-1} \mathbf{b}$.

Step III As mentioned in equation 6, the sufficient statistic $T(\mathbf{z}) = [\mathbf{z}; \text{vec}(\mathbf{z}\mathbf{z}^T)]$. In this case, the relationship equation 28 becomes:

$$\begin{pmatrix} \mathbf{z} \\ \mathbf{z}^2 \\ \mathbf{z}_{i,j} \end{pmatrix} = \mathbf{A} \begin{pmatrix} \hat{\mathbf{z}} \\ \hat{\mathbf{z}}^2 \\ \hat{\mathbf{z}}_{i,j} \end{pmatrix} + \mathbf{c}, \quad (29)$$

where $\mathbf{z}_{i,j}$ denote the vector whose elements are $z_i z_j$ for all $i \neq j$, \mathbf{A} in block matrix can be re-writed as:

$$\mathbf{A} = \begin{pmatrix} \mathbf{A}^{(1)} & \mathbf{A}^{(2)} & \mathbf{A}^{(3)} \\ \mathbf{A}^{(4)} & \mathbf{A}^{(5)} & \mathbf{A}^{(6)} \\ \mathbf{A}^{(7)} & \mathbf{A}^{(8)} & \mathbf{A}^{(9)} \end{pmatrix} \quad (30)$$

and \mathbf{c} as:

$$\mathbf{c} = \begin{pmatrix} \mathbf{c}^{(1)} \\ \mathbf{c}^{(2)} \\ \mathbf{c}^{(3)} \end{pmatrix}. \quad (31)$$

Then, we have:

$$\mathbf{z} = \mathbf{A}^{(1)} \hat{\mathbf{z}} + \mathbf{A}^{(2)} \hat{\mathbf{z}}^2 + \mathbf{A}^{(3)} \hat{\mathbf{z}}_{i,j} + \hat{\mathbf{c}}^{(1)}, \quad (32)$$

$$\mathbf{z}^2 = \mathbf{A}^{(4)} \hat{\mathbf{z}} + \mathbf{A}^{(5)} \hat{\mathbf{z}}^2 + \mathbf{A}^{(6)} \hat{\mathbf{z}}_{i,j} + \hat{\mathbf{c}}^{(2)}. \quad (33)$$

So we can write for each z_i :

$$z_i = \sum_j (A_{i,j}^{(1)} \hat{z}_j) + \sum_j (A_{i,j}^{(2)} \hat{z}_j^2) + \sum_{j \neq i} (A_{i,j}^{(3)} \hat{z}_i \hat{z}_j) + (c_i^{(1)}), \quad (34)$$

$$z_i^2 = \sum_j (A_{i,j}^{(4)} \hat{z}_j) + \sum_j (A_{i,j}^{(5)} \hat{z}_j^2) + \sum_{j \neq i} (A_{i,j}^{(6)} \hat{z}_i \hat{z}_j) + (c_i^{(2)}). \quad (35)$$

Squaring equation 34, we have:

$$z_i^2 = \underbrace{\left(\sum_j (A_{i,j}^{(1)} \hat{z}_j) \right)^2}_{(a)} + \underbrace{\left(\sum_j (A_{i,j}^{(2)} \hat{z}_j^2) \right)^2}_{(b)} + \underbrace{\left(\sum_{j \neq i} (A_{i,j}^{(3)} \hat{z}_i \hat{z}_j) \right)^2}_{(c)} + (c_i^{(1)})^2 + \dots \quad (36)$$

It is notable that equation 35 and equation 36 are derived from equation 28 which holds for arbitrary \mathbf{x} , then by the assumption (ii) in Theorem 4.1 that \mathbf{f} is a bijective mapping from \mathbf{z} to \mathbf{x} , and thus equation 35 and equation 36 must hold for \mathbf{z} everywhere. Then by the fact that the right sides of the equations equation 35 and equation 36 are both polynomials with finite degree, we have each coefficients of the two polynomials must be equal. In more detail, for the term (a) in Eq. equation 36:

$$\left(\sum_j (A_{i,j}^{(2)} \hat{z}_j^2)\right)^2 = \sum_j (A_{i,j}^{(2)})^2 \hat{z}_j^4 + \sum_{j \neq j'} (2A_{i,j}^{(2)} A_{i,j'}^{(2)} \hat{z}_j^2 \hat{z}_{j'}^2). \quad (37)$$

Compared with Eq. equation 35, since there is no term \hat{z}_j^4 in Eq. equation 35, we must have that:

$$\mathbf{A}^{(2)} = 0. \quad (38a)$$

For the term (c) in Eq. equation 36:

$$\left(\sum_{j \neq i} (A_{i,j}^{(3)} \hat{z}_i \hat{z}_j)\right)^2 = \sum_{j \neq i} (A_{i,j}^{(3)})^2 (\hat{z}_i \hat{z}_j)^2 + \dots \quad (39)$$

Compared with Eq. equation 35, since there is no term $(\hat{z}_i \hat{z}_j)^2$ in Eq. equation 35, we must have that:

$$\mathbf{A}^{(3)} = 0 \quad (40)$$

Similar, from the term (b), we have that

$$A_{i,j}^{(1)} A_{i,j'}^{(1)} = 0, \forall j \neq j', \quad (41)$$

The above equation indicates for each i , there are at most one j s.t. $A_{i,j}^{(1)} \neq 0$. There must be at least one j s.t. $A_{i,j}^{(1)} \neq 0$ (If $A_{i,j}^{(1)} = 0$ for all j , then z_i is a constant according to Eq. equation 34. That is, the sufficient statistic do not include z_i , which contradicts our assumption (iii)). As a result, the equation equation 34 can be simplified as follows:

$$z_i = (A_{i,j}^{(1)} \hat{z}_j) + (c_i^{(1)}). \quad (42)$$

A.2 THE PROOF OF THEOREM 5.1

The proof of Theorem 5.1 is similar to the proof of Theorem 4 in non-linear ICA Khemakhem et al. (2020). If the variational posterior $q(\mathbf{z}|\mathbf{x}, \mathbf{u})$ is large enough to include the true posterior $p(\mathbf{z}|\mathbf{x}, \mathbf{u})$, then by optimizing the loss, the KL term will be zero, and the loss will be equal to the log-likelihood. Since our identifiability is guaranteed up to permutation and scaling, the consistency of maximum log-likelihood means that we converge to the true latent causal variables up to permutation and scaling classes, in the limit of infinite data.

A.3 MORE RESULTS AND IMPLEMENTATION DETAILS

The recovered latent fMRI variables within one day by iVAE are depicted by Figure 8.

The recovered latent fMRI variables within one day by VAE are depicted by Figure 9.

The recovered latent fMRI variables within one day by β -VAE are depicted by Figure 10.

The recovered latent fMRI variables within one day by CausalVAE are depicted by Figure 11.

Implementation Details: We used the same network architecture for encoder (*e.g.* 3-layer fully connected network with 30 hidden nodes for each layer) and decoder (*e.g.* 3-layer fully connected network with 30 hidden nodes for each layer) parts in all these models. For prior model in the proposed SuaVE and iVAE, we use 3-layer fully connected network with 30 hidden nodes for each layer. We assign an 3-layer fully connected network with 30 nodes to generate the weights to model the relations among latent causal variables in the proposed SuaVE. For hyper-parameters, we set $\beta = 4$ for the β -VAE. For CausalVAE, we set the hyper-parameters as mentioned in the paper Yang et al. (2021).

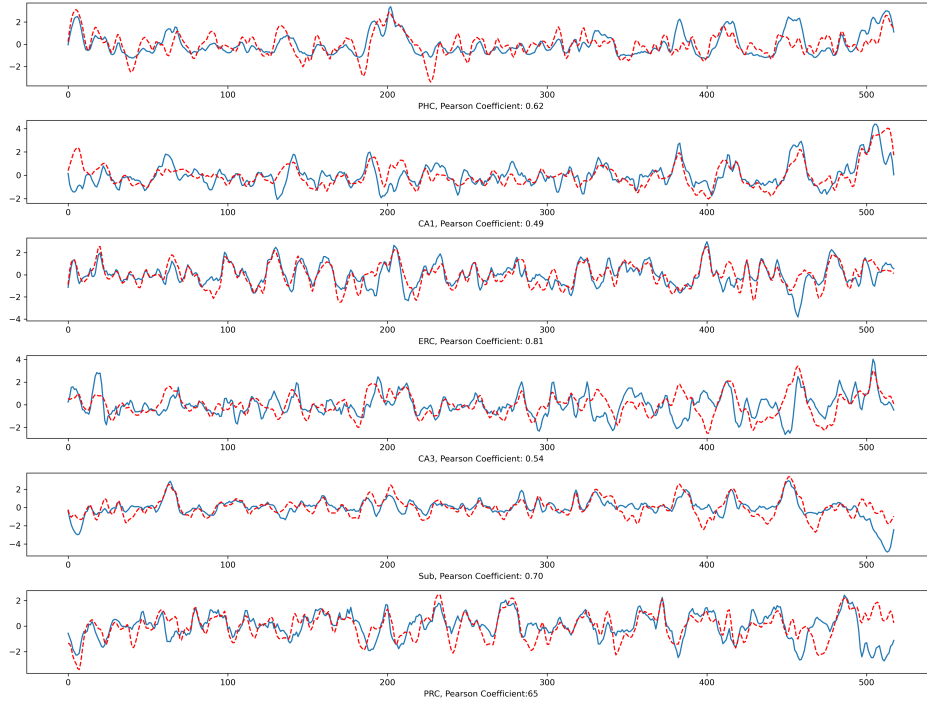


Figure 8: Recovered latent six signals (Blue) and the true ones (Red) within one day by iVAE.

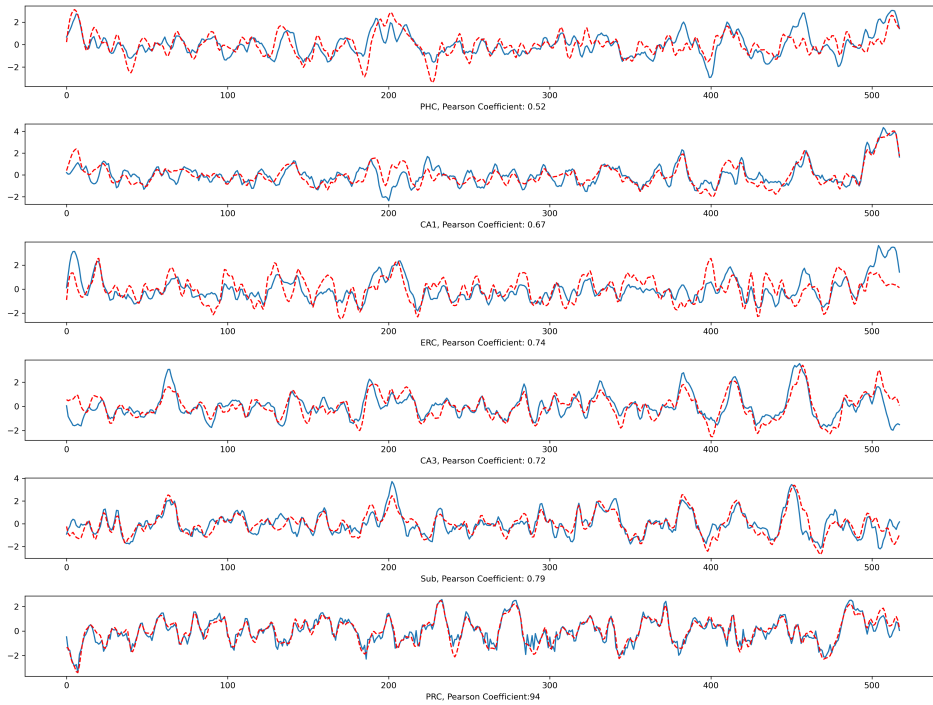


Figure 9: Recovered latent six signals (Blue) and the true ones (Red) within one day by VAE.

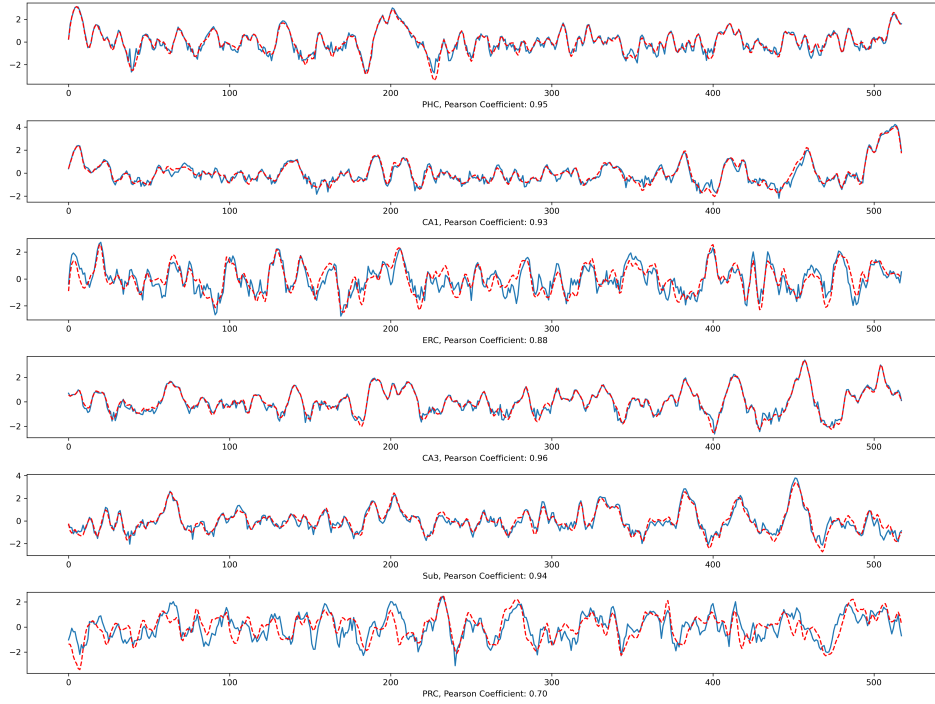


Figure 10: Recovered latent six signals (Blue) and the true ones (Red) within one day by β -VAE.

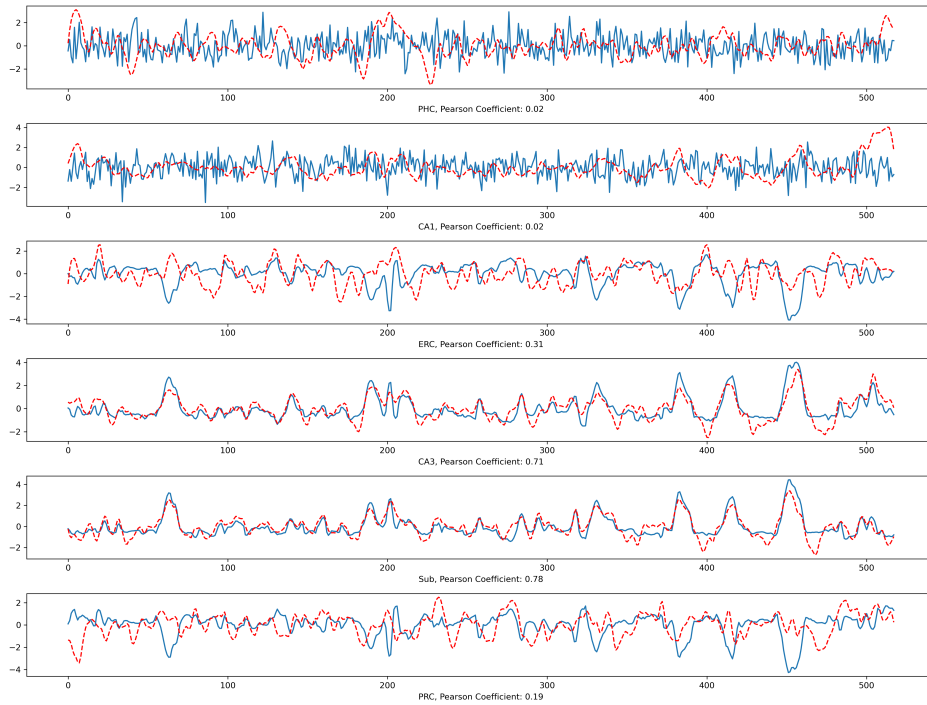


Figure 11: Recovered latent six signals (Blue) and the true ones (Red) within one day by CausalVAE.